Growth of the structure functions of deep inelastic scattering as the energy increases up to the unitarity limit

L. V. Gribov, E. M. Levin, and M. G. Ryskin

B. P. Konstantinov Leningrad Institute of Nuclear Physics, USSR Academy of Sciences
(Submitted 25 December 1980)
Zh. Eksp. Teor. Fiz. **80**, 2132–2148 (June 1981)

A method is developed for summing the quantum-chromodynamics perturbation-theory diagrams that contain for each power of the coupling constant $\alpha_s \ll 1$ at least one large logarithm, namely, $\ln q^2$, where q is the 4-momentum of the virtual photon, or $\ln \omega$ (where the energy ω is given by $\omega = 2(pq)/(-q^2)$, in which p is the 4-momentum of the target. The obtained system of equations makes it possible to calculate the structure functions $D(\omega, q^2)$ of deep inelastic scattering in an appreciably extended region of the leading logarithmic approximation: $\alpha_s^2(q_0^2) \ln \omega \ll \ln \ln q^2$, where q_0 is the momentum at which perturbation theory begins to be valid, and $\alpha_s(q_0^2) \ll 1$ [Eq. (15)]. It is shown that at large ω the multiladder diagrams (cuts in reggeon terminology) appreciably change the behavior of $D(\omega, q^2)$. With allowance for their influence, an expression is obtained for $D(\omega, q^2)$ in the region of ω not exceeding a certain limiting value $\omega_{\lim}(q^2)$, $\ln \omega < \ln \omega_{\lim} \propto 1/\alpha_s^2(q^2)$ [Eq. (29)]. It is shown that $D(\omega, q^2) \propto q^2$ at $\omega = \omega_{\lim}$, which corresponds to a constant cross section for absorption of the virtual photon.

PACS numbers: 11.20.Dj, 11.80.Fv

I. INTRODUCTION

In this paper, we study the behavior of the structure function $D(\omega, q^2)$ of deep inelastic scattering at superhigh energies, when the Bjorken variable $\omega = 2(pq)/(-q^2)$ is very large. In deep inelastic processes, the important region is that of short distances, where the coupling constant satisfies $\alpha_s \ll 1$, and we shall therefore operate in the framework of perturbation theory for quantum chromodynamics (QCD), separating the diagrams in which the smallness of α_s is compensated either by a large phase space $d\Omega \propto \ln \omega$, $\ln q^2$, or a high parton density $D(\omega, q^2)/\omega$.

Hitherto, the structure functions $D(\omega, q^2)$ have been calculated in a restricted region $\omega \sim$ const by summing the leading logarithms of the transverse momentum[1,2] [$\alpha_s(q_0^2) \ln(q_t^2/q_0^2) \sim 1$ but $\alpha_s(q_0^2) \ln \omega \ll 1$; region A in Fig. 1]. In addition, the structure of the vacuum singularity (i.e., the behavior at large ω) of QCD was investigated by Kuraev *et al.*,[3] who succeeded in summing the logarithms of the longitudinal momenta in the region $\alpha_s(q_0^2) \ln \omega \sim 1$ but $\alpha_s(q_0^2) \ln(q_t^2/q_0^2) \ll 1$ (B in Fig. 1). Now in both cases the problem reduces in a physical gauge in which only transverse gluon polarizations propagate (for example, in a planar gauge) to the consideration of ladder diagrams (Fig. 2a), and this has made it possible for us to sum the logarithms of both types and appreciably extend the region of applicability of the leading logarithmic approximation of QCD. The condition of applicability of the leading logarithmic approximation is now $\alpha_s^2(q_0^2) \ln \omega \ll 1$. The second section of the paper is devoted to this.

When ω increases, so does the density $D(\omega, q^2)$ of the partons, and they begin to screen each other. The characteristic parameter ζ that determines the probability of interaction of partons from different ladders is

$$\zeta = \alpha_s D(\omega, q^2)/\omega q^2.$$

As a result, even for $\alpha_s \ll 1$, it is necessary in the region of very large $\ln \omega$,

$$\ln \omega > \ln [\alpha_s(q_0^2)/\alpha_s(q^2)]/\alpha_s^2(q_0^2),$$

when $\zeta \sim 1$, to take into account not only the leading logarithmic approximation but also multiladder diagrams (cuts in the language of complex angular momenta). In the third section, we discuss the structure of such diagrams, and we show that in a wide range of $\ln \omega < 1/\alpha_s^2(q^2)$ the influence of the cuts reduces to the imposition of a new boundary condition in the principal ladder equation of the leading logarithmic approximation [$\zeta \propto \alpha_s(q^2)$ on the line $\ln \omega = 0.42\pi^2/N\beta_2\alpha_s^2(q^2)$: curve 2 in Fig. 1], and we investigate the behavior of the structure functions at these large ω.

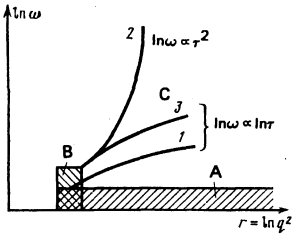

FIG. 1.

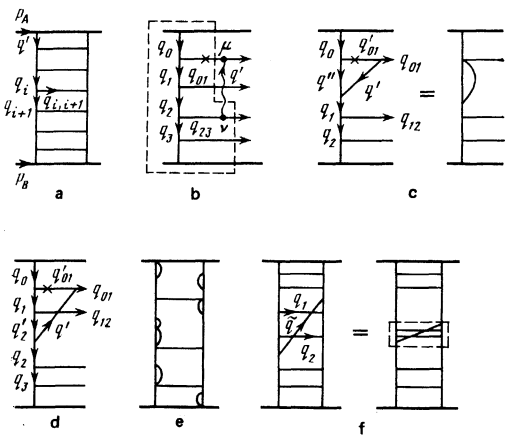

FIG. 2.

 0038-5646/81/061113-09$02.40

II. EQUATIONS OF THE LEADING LOGARITHMIC APPROXIMATION WITH ALLOWANCE FOR TWO LARGE LOGARITHMS

1. Selection of diagrams

It is well known that diagrams in which there is a logarithm of the transverse momentum (or q^2, the "virtuality") at each power of α_s have ladder structure[1,2] in any physical gauge (in particular a planar gauge) in which only transverse gluon polarizations propagate.[4] Moreover, the self-energy graphs and the corrections to the vertices change the unrenormalized $\alpha_s(\mu^2)$ into the running coupling constant $\alpha_s(q^2)$.

On the other hand, it has been shown[3] that all longitudinal logarithms ($\ln\omega$) can be collected together by summing the ladder graphs in which the exchange in the t channel is realized by a reggeized gluon. This fact will enable us in the second part of this section to find a system of Bethe–Salpeter type equations that sums all graphs containing at each power of α_s at least one large logarithm, namely, $\alpha_s \ln\omega$ or $\alpha_s \ln q^2$, or both at once: $\alpha_s \omega \ln q^2$.

For greater clarity and also to permit in what follows an estimate of the accuracy of our calculations, we shall now show that after a certain gauge transformation the diagrams which collect together the longitudinal logarithms acquire a ladder structure, and the graphs concentrated entirely within one cell of the ladder correspond to gluon reggeization.

We consider the first corrections ($\sim\alpha_s$) to the $(2\to n)$ amplitude for the production of n particles as shown in Fig. 2b; these corrections describe reggeization of gluons with momenta q_1 and q_2 (1 and 2) in the t channel.[3] We introduce the Sudakov variables[5]

$$q_i=\alpha_i p_A+\beta_i p_B+q_{it}$$

and, using the device of Ref. 6, express the total contribution of the graphs in Fig. 2b by means of the Ward identities in terms of the contributions of the diagrams concentrated entirely within the same cell (2). Suppose a gluon with momentum q' is emitted from line q_{01} and absorbed at some other point of the ladder; we close the contour of integration with respect to β' around the pole $1/q_{01}^2$ (for case 2b). One integration over q', longitudinal logarithms arise only because of the longitudinal part of the gluon spin matrix $g_{\mu\nu}\approx p_{B\mu}p_{A\nu}/(p_A p_B)$. By virtue of the gauge invariance of the block in Fig. 2b surrounded by the broken line,

$$M_\nu q_\nu'=M_\nu(\alpha' p_A+\beta' p_B+q_t')_\nu=0,$$

the momentum $p_{A\nu}$ in the propagator $p_{B\mu}p_{A\nu}/(p_A p_B)$ can be replaced by $-q_{t\nu}'/\alpha'$ and, similarly, $p_{B\mu}$ by $-q_{t\mu}'/\beta'$. As a result, in the spin part $2q_{t\mu}'q_{t\nu}'/\alpha'\beta's$ of the q' gluon propagator an extra power of $1/\alpha'$ arises. Making the substitution $p_{B\mu}p_{A\nu}\to q_{it\mu}q_{it\nu}/\alpha_i\beta_i$ in the propagators of the gluons q_1 and $q_2,\ldots$, we see that even in the most advantageous region $\alpha_1\gg\alpha'\gg\alpha_2$ the integral over the $d\alpha'$ takes the form $(\alpha_2/\alpha')^2 d\alpha'/\alpha'$ (in this region, $q_{23}^2\approx\alpha'\beta_3 s$) and, of course, it does not give $\ln\omega$. The only exceptions are graphs of self-energy or vertex part type concentrated within one cell (Fig. 2c). Indeed, closing the contour with respect to β' once more around the pole $1/q_{01}'^2$ ($\beta'=(q_{01t}'^2-q_{01t}^2)/\alpha_0 s$), we see that the largest contribution is made by the configurations for which $g_{\mu\nu}^\perp$ is left in the numerator in one of the propagators of the gluons q' and $q''=q_1-q'$ and in the other, say q', the term $p_{A\mu}p_{B\nu}/(p_A p_B)=2q_{t\mu}'q_{t\nu}'/\alpha'\beta's$ is left. [It is not advantageous to replace $g_{\mu\nu}$ by $2q_{t\mu}'q_{t\nu}'/\alpha'\beta's$ in all the propagators, since the product of the three-gluon vertex $\Gamma_{\mu\nu\delta}(q',q'',q_1)$ by its transverse momenta vanishes, $\Gamma_{\mu\nu\delta}(q',q'',q_1)q_{\mu t}'q_{\nu t}''q_{1\delta t}'=0$.] As a result, we obtain the logarithmic integral

$$\frac{d\alpha'}{\alpha_0 s}\frac{q_t'}{\alpha'}\frac{q_t'}{\beta'}\propto\frac{d\alpha'}{\alpha'}\frac{q_t'^2}{q_{01t}'^2-q_{01t}^2},$$

which corresponds to reggeization of the gluon q_1^3. Any other diagram encompassing several rungs (for example, Fig. 2d) will not contain longitudinal logarithms.

In the region $\alpha_0\gg\alpha'\gg\alpha_1$, the propagator of the gluon q_2' introduces an extra factor $1/\alpha'\beta_2 s=\alpha_1/\alpha' q_{12t}^2$, which destroys the logarithmic nature of the integration over α'. There remains the region $\alpha_1\gg|\alpha'|\gg\alpha_2$. For negative α', the contour with respect to β' can be closed around the poles $1/q_{01}'^2$, $1/q'^2$, and $1/(q_2-q')^2$, and for positive α' there remains only the single pole $1/q_{01}'^2$ in the upper half-plane of β'. The contributions of this pole in the intervals $-\alpha_1\ll\alpha'\ll-\alpha_2$ and $\alpha_1\gg\alpha'\gg\alpha_2$ cancel each other. The poles $1/q'^2$ and $1/(q_2-q')^2$ do not lead to logarithmic integrals over α' because the gluons are highly virtual:

$$q_1^2\approx\alpha_1\beta' s=(\alpha_1/\alpha')q_t'^2,\quad q_{01}'^2\approx-\alpha_0\beta' s=-(\alpha_1/\alpha')q_t'^2.$$

Thus, using the gauge invariance (i.e., canceling the diagrams with longitudinal polarization of the gluon $q'-q_\mu'$), we have been able to calculate the total contribution of the diagrams of the type in Fig. 2b corresponding to reggeization in terms of the contribution of diagrams of ladder form: Fig. 2e.[1)] Integration with respect to the transverse momentum q_t' in these graphs gives the trajectory of the reggeized gluon $\alpha_G(q^2)=j_G-1$ obtained in Ref. 3. By a similar method, separating the transverse physical polarizations and replacing $p_{A\nu}p_{B\mu}$ by $q_{it\nu}q_{it\mu}/\alpha_i\beta_i$, we can show that only $(2\to n)$ amplitudes of comb type, i.e., the ladder diagrams in Fig. 2a, give longitudinal logarithms on integration with respect to the momenta of the newly created particles. Moreover, the resulting square of the emission vertex for the following gluon exactly reproduces the sum of the contributions of all the diagrams containing the corresponding $\ln\omega$ in the case of the Feynman gauge. Since the transverse logarithms $\ln q^2$ can also be contained only in ladder graphs, we can, summing the ladder diagrams of the types in Figs. 2a and 2e, calculate the structure functions $D(\omega,q^2)$ of deep inelastic scattering to accuracy $O(\alpha_s^2\ln\omega)$.

Indeed, no extra (not taken into account in our diagrams) gluon (see Fig. 2f) gives a single logarithm on integration with respect to its momentum but merely introduces an additional small α_s, and the number of cells in which this extra gluon can be drawn is $\approx\alpha_s\ln\omega$. Moreover, if this extra gluon intersects several cells, its momentum $\tilde{q}$ simultaneously destroys

the logarithmic nature of the integrations with respect to the momenta q_2 of the cells it traverses. The point is that the ladders in Figs. 2a and 2e are on the average white (color singlets). As a result, there is no charge emission of long-wavelength gluons ($\tilde{q} \ll q_2$), and the dipole (and higher multipole) radiation contains the small ratio $\sim \tilde{q}/q_2$. It is this factor $\tilde{q}/q_2$ that destroys the logarithmic nature of the integrations with respect to the momentum $\tilde{q}$ and simultaneously with respect to the momentum q_2. As a result, the characteristic values of the momenta $\tilde{q}$ and q_2 are of order q_1, and the entire block surrounded by the broken line in Fig. 2f can be regarded as a "point" kernel ΔK of a ladder diagram (of higher order in α_s), the kernel describing the emission of an entire system of quarks and gluons with nearly equal momenta $\tilde{q} \sim q_2 \sim q_1$.

Thus, to calculate the structure function $D(\omega, q^2)$ we must find the sum of the ladder graphs in Figs. 2a and 2e, and to estimate the accuracy of the calculations it is sufficient to consider how the result is changed by the addition to the kernel K of the ladder equation of a correction $\Delta K \sim O(K\alpha_s)$.

2. Derivation of the system of equations

Since the angular momentum j is conserved along the ladder, it is convenient to sum the graphs of Fig. 2a in the j, q^2 representation:

$$\varphi(j, q^2) = \int \varphi(\omega, q^2)\, \omega^{-j} d\omega.$$

To make the gluons and quarks occur on an equal footing in our equations, we shall not use the structure function $D(\omega, q^2)$ but the functions $\varphi_F(\omega, q'^2)$ (respectively, φ_G), which correspond to the cross sections of the processes in Fig. 2a when we fix in the uppermost cell a quark (respectively, gluon) with definite transverse momentum q_t':

$$D(\omega, q^2) = \omega \int^{q^2} \varphi_F(\omega, q'^2)\, dq'^2. \tag{1}$$

The system of equations that describes the variation of the functions $\varphi(j, q'^2)$ with increasing q'^2 has the form (Fig. 3)

$$\varphi_G(j, q^2) = \int^{q^2} \left[\frac{4NK(q^2, q'^2)}{j-1} \varphi_G(j, q'^2) + \frac{4C_2 \varphi_F(j, q'^2)}{q^2(j-1)} \right] \frac{\alpha_s(q'^2)}{4\pi} dq'^2$$
$$+ \int^{q^2} [\Phi_G^G(j) \varphi_G(j, q'^2) + \Phi_F^G(j) \varphi_F(j, q'^2)] \frac{\alpha_s(q'^2)}{4\pi} \frac{dq'^2}{q^2}, \tag{2}$$
$$\varphi_F(j, q^2) = \int^{q^2} [\Phi_F^F(j) \varphi_F(j, q'^2) + 2n_F \Phi_G^F(j) \varphi_G(j, q'^2)] \frac{\alpha_s(q'^2)}{4\pi} \frac{dq'^2}{q^2},$$

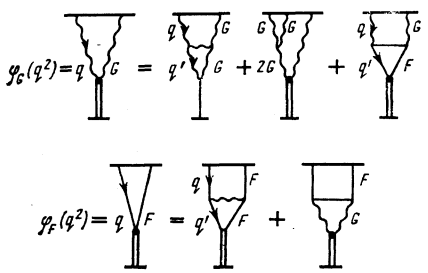

FIG. 3.

where $N = 3$ is the number of colors, $C_2 = (N^2 - 1)/2N$, and n_F is the number of quark species. Because the spin of a quark is $\frac{1}{2}$, the cells with exchange of a fermion do not contain a singularity as $j \to 1$ (i.e., $\ln \omega$). Therefore, all terms proportional to $1/(j-1)$ are concentrated in the first equation of the system (2), which describes cells with gluon exchange. The purely gluon cells are described by the kernel $K(q^2, q'^2)$ (Ref. 3):

$$K(q^2, q'^2)\varphi(q'^2) = \frac{\varphi(q'^2)}{(q-q')_t^2} - \frac{q_t^2 \varphi(q^2)}{(q-q')_t^2 [q_t'^2 + (q-q')_t^2]} \tag{3}$$

where the first term corresponds to the emission of one further gluon with momentum $q - q'$, and the second takes into account, by virtue of the identity

$$\frac{N\alpha_s}{2\pi^2} \int \frac{d^2 q_t' (q_t^2 - m^2)}{[(q'-q)_t^2 - m^2][(q'-q)_t^2 + q_t'^2 - 2m^2]} = \alpha_s(q_t^2),$$

the reggeization of the gluons [with trajectory $j_G = 1 + \alpha_G(q_t^2)$]. We emphasize that from the point of view of the integration with respect to the transverse momentum q_t' the kernel K(3) has been written down exactly.

The remaining kernels Φ_G^G, Φ_F^G, etc., describe cells in which a logarithm of the transverse momentum arises but not $\ln \omega$. These kernels are identical to the kernels $\tilde{\Phi}$ given in Refs. 1 and 9 if we separate from the kernels $\tilde{\Phi}$ the singularity $1/(j-1)$, which is already included in the kernel K. We have

$$\Phi_G^G(j) = \int_0^1 dz \left\{ 4N \left(z - z^2 - 2 + \frac{1}{1-z} \right) z^{j-1} - \frac{4N}{1-z} \right\}$$
$$- \frac{2n_F}{3} + \frac{11N}{3} \to -\frac{11N}{3} - \frac{2n_F}{3} \quad \text{as } j \to 1,$$
$$\Phi_F^F(j) = C_2 \int_0^1 \left\{ \frac{2(1+z^2)}{1-z} z^{j-1} - \frac{4}{1-z} \right\} dz + 3C_2 \to 0 \quad \text{as } j \to 1, \tag{4}$$
$$\Phi_F^G = C_2 \int_0^1 dz z^{j-1}(2z-4) \to -3C_2 \quad \text{as } j \to 1,$$
$$\Phi_G^F = \int dz z^{j-1}(z^2 + (1-z)^2) \to \frac{2}{3} \quad \text{as } j \to 1.$$

For example, the sum of the second and fourth terms of the first equation of the system (2) gives $4C_2/(j-1) + \Phi_F^G = \tilde{\Phi}_F^G$, where $\tilde{\Phi}_F^G$ is the kernel calculated in Refs. 1 and 9. Since cells with exchange of a quark contain only a logarithm of the transverse momentum, the right-hand side of the equation for φ^F can be expressed solely in terms of the kernels Φ_G^F and Φ_F^F, and $\Phi_G^F = \tilde{\Phi}_G^F$ and $\Phi_F^F = \tilde{\Phi}_F^F$. Strictly speaking, in Eqs. (2) we should add an inhomogeneous term, which is a function which decreases faster than $1/q^2$ for $q^2 \gg m^2$. Instead of this, we shall seek the solution for the region $q^2 > q_0^2 \gg m^2$, representing it in the form of the integral (12) with respect to the eigenfunctions of the homogeneous system (2) and find the expansion coefficients using the boundary condition at the point $q^2 = q_0^2$.

3. Solution of the system (2)

If the coupling constant α_s did not depend on q^2, Eqs. (2) would be homogeneous in the arguments q^2 and q'^2. Then the eigenfunctions of the system (2) would have the form

$$\varphi_f(q^2)=(q^2)^{f-1},$$

and

$$\int K(q^2,q'^2)\varphi_f(q'^2)\,dq'^2=\chi(f)\varphi_f(q^2),$$
$$\chi(f)=-2C_E-\psi(f)-\psi(1-f) \tag{5}$$

(for more details, see Ref. 3); C_E is Euler's constant, $\psi(f)=d\ln\Gamma(f)/df$, $\Gamma(f)$ is the gamma function. Using this remark and substituting in (2) the explicit expression for $\alpha_s(q^2)$,

$$\alpha_s(q^2)=\frac{4\pi}{\beta_2\ln(q^2/\mu^2)}=\frac{4\pi}{\beta_2 r}$$

$[\beta_2=\frac{11}{3}N-\frac{2}{3}n_F,\ r=\ln(q^2/\mu^2]$, we shall seek the solution in the form

$$\varphi_{G,F}(j,q^2)=\int A^{G,F}(f)\exp\Big[(j-1)r-\frac{4N}{\beta_2(j-1)}\int^f\chi(f')\,df'\Big]\frac{r\,df}{2\pi}. \tag{6}$$

By means of relations obtained by integration by parts,

$$\int I'(f)A(f)\exp(fr-I(f))\,df$$
$$=\int A(f)\exp(fr-I(f))\,r\,df+\int A'(f)\exp(fr-I(f))\,df,$$
$$r\int A(f)\exp(fr-I(f))\,df=\int\exp(fr-I(f))\,[A(f)I'(f)-A'(f)]\,df; \tag{7}$$
$$A'=\frac{dA}{df},\quad I(f)=\frac{4N}{\beta_2(j-1)}\int^f\chi(f')\,df'$$

we readily find equations for the expansion coefficients $A(f)$:

$$-\beta_2 fA'^G=\Phi_G{}^GA^G+A^F[\Phi_F{}^G+4C_2/(j-1)],$$
$$-\beta_2 fA'^F=2n_F\Phi_G{}^FA^G+A^F[\Phi_F{}^F-4Nf\chi(f)/(j-1)]. \tag{8}$$

In the region of large ω, i.e., $j-1\ll 1$, in which we are most interested, the system (8) has the obvious solution

$$A^F(f)=2n_F\Phi_G{}^FA^G(f)\,(j-1)/4Nf\chi(f),$$
$$A^G(f)=\text{const}\cdot\exp\Big[-\frac{\ln f}{\beta_2}\Big(\Phi_G{}^G+\frac{2C_2n_F\Phi_G{}^F}{Nf\chi(f)}\Big)\Big]. \tag{9}$$

In the case of finite ω, the values of $f\approx 4N/\beta_2 r(j-1)$ important in the integrals (6) are very small. This makes it possible to simplify Eq. (8) by expanding the function $\chi(f)$ in powers of f: $f\chi(f)=1+O(f^3)$ as $f\to 0$. Then the solutions of the system (8) take the form

$$A^G(f)=A_0{}^Gf^\gamma,\quad A^F(f)=A_0{}^Ff^\gamma, \tag{10}$$

where

$$A_0{}^F=\frac{A_0{}^G2n_F\Phi_G{}^F}{4N/(j-1)-\gamma\beta_2-\Phi_F{}^F},$$

and γ satisfies the equation

$$\gamma^2-\frac{\gamma}{\beta_2}\Big[\frac{4N}{j-1}-\Phi_G{}^G-\Phi_F{}^F\Big]=\frac{2n_F}{\beta_2{}^2}\Phi_G{}^F\Big[\Phi_F{}^G+\frac{4C_2}{j-1}\Big]+\frac{\Phi_G{}^G}{\beta_2{}^2}\Big[\frac{4N}{j-1}-\Phi_F{}^F\Big]. \tag{11}$$

For numerically large ω, when $j-1\ll 1$, the solution (10) coincides with (9), since in the limit $j\to 1$

$$\gamma\to-\frac{1}{\beta_2}\Big[\Phi_G{}^G+\frac{2n_FC_2}{N}\Phi_G{}^F\Big],\quad f\chi(f)|_{f\ll 1}=1.$$

Therefore, to good accuracy we can use the solution (10), (6) in the complete range of j (or ω). It only remains to choose the coefficients $A_0^G(j)$ to satisfy the initial conditions for some fixed but large $q^2=q_0^2(\alpha_s(q_0^2)\ll 1)$:

$$\varphi(\omega,q^2)=\int\varphi(j,q^2)\omega^{j-1}\frac{dj}{2\pi i}=\iint A_0(j)rf^\gamma\exp\Big\{(j-1)\ln\omega$$
$$+(j-1)r-\frac{4N}{\beta_2(j-1)}\int_{0,5}^f\chi(f')\,df'\Big\}\frac{df\,dj}{2\pi 2\pi i}\Big|_{q^2=q_0^2}=\varphi_0(\omega,q_0^2). \tag{12}$$

At large ω and q_0^2, the integrals (12) can be conveniently calculated by the method of steepest descent. The saddle-point value f_0 is determined from the solution of the equation

$$\frac{\beta_2r^2}{4N\ln\omega}=\chi^2(f_0)\Big/\int^{f_0}\chi(f')\,df',\quad j_0-1=\Big[-\frac{4N}{\beta_2\ln\omega}\int^{f_0}\chi(f')\,df'\Big]^{1/2}. \tag{13}$$

It can be seen from this that $A_0(j)$ is determined by the value of $\varphi_0(\omega_0,q_0^2)$ at

$$\ln\omega_0=-\frac{4N}{\beta_2(j-1)^2}\int^{f_0}\chi(f')\,df'\approx\frac{4N}{\beta_2(j-1)^2}\ln\Big[\frac{\beta_2}{4N}r(j-1)\Big],\quad \ln\omega_0\ll r_0^2,$$

and this coefficient $A_0(j)$ determines the function $\varphi(\omega,q^2)$ simultaneously on the entire line $j=\text{const}$, i.e.,

$$\ln\frac{\omega}{\omega_0}\approx\frac{4N}{\beta_2(j-1)^2}\ln\Big[\frac{\ln(q^2/\mu^2)}{\ln(q_0^2/\mu^2)}\Big] \tag{14}$$

(curve 1 in Fig. 1). Substituting the values of the coefficients $A_0(j)$ found in this way in a solution of the system of equations (2) of the form (12), we can calculate the structure functions of deep inelastic processes in a wide range:

$$\alpha_s^2(q_0^2)\ln\omega\ll\ln[\alpha_s(q_0^2)/\alpha_s(q^2)]. \tag{15}$$

The restriction (15) is due to the fact that the system (2) does not take into account the corrections $\Delta K\sim\alpha_s$ to the ladder kernels K, i.e., the terms proportional to $\alpha_s^2\ln\omega$ must be small.

4. Discussion of the corrections

To get a better feeling for the part played by the corrections to the ladder kernels, we consider the simplified equation

$$\varphi(j,q^2)=\frac{N}{\pi(j-1)}\int K(q^2,q'^2)\varphi(j,q'^2)\alpha_s(q'^2)\,dq'^2, \tag{16}$$

in which we retain from the system (2) only the term singular in j (the most dangerous at large $\ln\omega$). In the case of the simplest kernel $K=O(1)$ [see (3)] a solution of (16) is the function

$$\varphi=\int A(f)r\exp\Big[(j-1)r-\frac{4N}{\beta_2(j-1)}\int^f\chi(f')\,df'\Big]\frac{df}{2\pi},$$

where $A'(f)=0$, i.e., $A(f)=\text{const}$.

We add to the kernel K the correction $\Delta K=O(1)$ the $=O(\alpha_s(q^2))$.[2] Since the coupling constant in QCD is dimensionless, the term $\Delta K/\alpha_s$ is also a homogeneous function of the arguments q^2 and q'^2. Therefore,

$$\int\frac{\Delta K(q^2,q'^2)}{r}(q'^2)^{f-1}\,dq'^2=q^{2(f-1)}\Delta\chi(f),$$

and, since all the integrals logarithmic in q_i^2 have already been taken into account, the ratio $\Delta\chi(f)/\chi(f)$ in the system (2) does not have singularities with respect to f as $f\to 0$.

The equation for the coefficients $A(f)$ now takes the

form

$$A''-\frac{4N}{\beta_2(j-1)}[A'\chi(f)+A\Delta\chi(f)]=0, \qquad (17)$$

and in our region $j-1\ll 1$

$$A(f)=\text{const}\cdot\exp\left[-\int^{f}\frac{\Delta\chi(f')}{\chi(f')}df'\right]$$

or, for small f,

$$A(f)\propto\exp\left[-f\frac{\Delta\chi}{\chi}\Big|_{f\to 0}\right].$$

Thus, the influence of the following α_s corrections to the ladder kernel $K(3)$ becomes important only at r and $\ln\omega$ values for which the characteristic saddle-point values satisfy $f=f_0\to 0(1)$ [see (13)]. From this point of view, the most dangerous point on the trajectory with given $j=\text{const}$ [see (14)] is the initial point. Indeed, along the trajectory (14) $\ln\omega$ increases much more slowly than $1/\alpha_s^2(q^2)$, so that at ω_0, q_0 the value of f is maximal, and f decreases with a further increase in q^2. From this the restriction (15) arises. In principle, the correction $\Delta\chi(f)$ can be calculated and one can then specify the exact values of $A(f)$ in the complete f interval. However, even where $f=O(1)$ the coefficients $A(f)$ do not change too rapidly [by several times compared with $A(0)$]. Such a change of $A(f)$ can be regarded as a renormalization of $A(0)$ at the start of the trajectory. Therefore, without pretending to the exact finding of the pre-exponential factor, we pose the problem of the behavior of the functions $\varphi(\omega,q^2)(\ln\varphi)$ in the much larger region $\ln\omega\lesssim\alpha_s^{-2}(q^2)$.

Unfortunately, we here cannot restrict ourselves to the solution of the relatively simple system of equations (2), since when $\ln\omega$ increases the density of partons rapidly grows and one must take into account their mutual screening, coalescence (of two into one), and mutual multiple scattering.

III. REABSORPTION AND SCREENING OF PARTONS

1. The simplest diagrams

We consider how the parton density $D(\omega', q'^2)/\omega' \propto q'^2\varphi(\omega', q'^2)$ changes as the virtuality q'^2 increases along the ladder in Fig. 2a or, which is the same thing, along the trajectory with given j (14).

As follows from the relations (13), $\beta_2 r(j-1)=4N\chi(f_0)$, i.e.,

$$\frac{\partial f_0}{\partial r}\Big|_{j=\text{const}}=\frac{\beta_2(j-1)}{4N\chi'(f_0)}<0,$$

$$\frac{\partial\ln\omega}{\partial r}\Big|_{j=\text{const}}=-\frac{4N\chi(f_0)}{\beta_2(j-1)^2}\frac{\partial f_0}{\partial r}=-\frac{\chi(f_0)}{\chi'(f_0)(j-1)}.$$

Substituting these expressions in Eq. (12), we obtain

$$-k=\frac{\partial\ln\varphi}{\partial r}\Big|_{j=\text{const}}=f_0-1-\frac{\chi(f_0)}{\chi'(f_0)}+O(\alpha_s), \qquad (18)$$

where $f-1-\chi(f)/\chi'(f)=0$ at $f=0.37$.

It can be seen from (18) that for $f>0.37$ the derivative $-k$ is positive, $-k>0$. This means that for sufficiently small $j-1$ the function φ initially increases exponentially fast with τ, and it is only when r has increased so much that f_0 becomes less than 0.37 (corresponding to $\Delta r=r-r_0\sim r_0$) that φ begins to decrease. At the same time, the parton density in the ladder comb $D(\omega,q^2)/\omega\propto q^2\varphi=e^r\varphi$ increases monotonically with increasing virtuality. Since the transverse momenta also increase along the ladder (in the direction from the target to the virtual photon), there is no diffusion in the space of the impact parameters $b_\perp$, and all the partons are concentrated in a region of the order of the geometrical dimensions of the target, $\langle b_\perp^2\rangle\sim R_{tg}^2$. Each particle with virtuality q^2 occupies the area $\sim 1/q^2$, and the interaction cross section of such particles is $\sigma(gg)\sim\alpha_s/q^2$. It is therefore natural to expect that once the parton density D/ω exceeds the value $R_{tg}^2/\sigma(gg)$ the partons will begin to coalesce and screen one another. Indeed, in this region $[D/\omega > R_{tg}^2/\sigma(gg)$, i.e., $\alpha_s(q^2)\varphi(\omega,q^2)>1]$ multiladder diagrams (multipomeron cuts) describing screening processes come into play. The first diagram which becomes effective is the one in Fig. 4a.

Since the vertex for the coalescence of two ladders into one (Fig. 4b) contains an extra coupling constant $\alpha_s(q'^2)$, which does not give rise to any logarithm, the consideration of such graphs takes us out of the framework of the leading logarithmic approximation [as does allowance for the corrections $\Delta K\sim\alpha_s$ in the kernel of the ladder equations (2)]. But since here the small quantity $\alpha_s(q'^2)$ is multiplied by the large $\varphi(\omega', q'^2)$, such diagrams play a fundamental part in the region C (to the left of curve 2 in Fig. 1), where the cross section for interaction of the virtual gluon (quark) with the target is $\sigma(q'^2)\sim\alpha_s(q'^2)\varphi(\omega', q'^2)$ and comparable with the target area πR_{tg}^2.

We turn to the graph in Fig. 4a and choose a point ω', q' lying on the trajectory along which the ladder (1, 2) develops, i.e., $j(\omega', q')=j(\omega,q)=\text{const}$. By making this choice of the point ω', q' we have in no way spoilt the integrations within this ladder. As can be seen from Fig. 4a, the integration with respect to the transverse momentum q_{Rt} running through the reggeons[3] 2 and 3 is cut off by the target form factor, i.e., the characteristic values are $\langle q_{Rt}^2\rangle\sim 1/R_{tg}^2$. As a result, the contribution of the sum of the diagrams 2a and 4a can be represented in the form

$$J_{2a}+J_{4a}=\varphi(\omega,q^2)[1-G_{\text{eff}}\langle q_{Rt}^2\rangle\alpha_s(q'^2)\varphi(\omega', q'^2)/16\pi^2], \qquad (19)$$

where $\alpha_s(q'^2)G_{eff}$ is the effective three-pomeron vertex (of coalescence of two ladders into one) described by the sum of the graphs in Fig. 4b. For what follows,

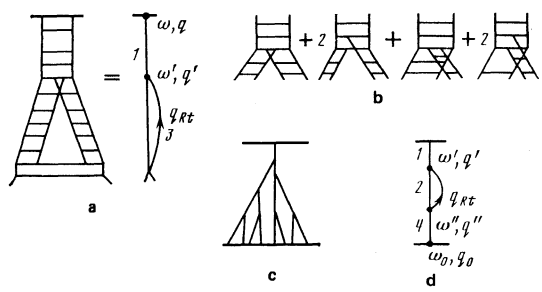

FIG. 4.

we only need to know that at $q_{Rt}^2 \ll q'^2$ i.e., at small momentum transfers through the reggeons, the value of G_{eff} tends to a constant limit $G_{eff}(q_{Rt}^2 \to 0) \to \text{const}$. The contribution J_{4a} [the second term in (19)] reaches its greatest value at $r' = \ln q'^2$ values for which the corresponding $f_0' = 0.37$, i.e., when the function $\varphi(\omega', q'^2)$ is maximal. We emphasize that the condition $q_{Rt}^2 \ll q'^2$ is satisfied in the self-consistent calculation of the semienhanced diagrams of the type of Fig. 4c irrespective of the target form factor.

Indeed, if the value of q_{Rt} is large, $q_{Rt} > 1/R_{tg}$, then the smallest "initial" virtualities within the reggeons 2 and 3 will be determined by q_{Rt}^2, and it is these virtualities that limit the geometrical size of the region of impact parameters $\langle b_\perp^2 \rangle$ in which our partons are concentrated ($\langle b_\perp^2 \rangle \sim 1/q_{Rt}^2$). Thus, q_{Rt}^2 in the case of large q_{Rt} plays the part of a reciprocal "size" of the target. On the other hand, as will be shown below, the summation of the graphs in Fig. 4c halts the growth of the functions $\varphi(\omega', q')$ (when ω increases) at the level $\varphi = \varphi_{max} \sim \langle b_\perp^2 \rangle / \alpha_s(q'^2)$, when the probability of parton reabsorption

$$w \sim D(\omega', q'^2)\sigma(gg)/\omega' \langle b_\perp^2 \rangle \sim \alpha_s \varphi / \langle b_\perp^2 \rangle$$

becomes of order unity. As a result, the functions $\varphi(\omega', q'^2, q_{Rt}^2)$ corresponding to the reggeons 2 and 3 decrease with increasing q_{Rt} as $1/q_{Rt}^2$ in the same interval of values of the arguments ω' and q' in which the contribution J_{4a} [the second term in the expression (19)] ceases to be negligibly small compared with J_{2a}.

Then the integral over the momentum transfer q_{Rt} takes the form

$$\int_{q''} \varphi^2(\omega', q'^2, q_{Rt}^2)\, d^2 q_{Rt} \propto \int_{q''} d^2 q_{Rt}/q_{Rt}^4 = \pi/q''^2.$$

It can be seen from this that the important values of q_{Rt} are determined by the lower limit of integration q'', i.e., either by the initial virtuality or by the size of the target itself[4]: $1/R_{tg}$.

The contribution of the completely enhanced diagram of Fig. 4d, J_{4d}, is less than J_{4a} since in the graph of Fig. 4d the section from r_0 to r'', on which the function $\varphi(\omega', q')$ increased exponentially in the diagram of Fig. 4a, is not used (the estimate of the characteristic momenta q_{Rt} transferred through the reggeons 2 and 3 here repeats literally the case 4a.)

Thus, we have seen that once the maximal value of $\varphi(\omega', q')$ somewhere within the ladder [i.e., somewhere on the trajectory (14) with given $j(\omega', q') = \text{const}$] reaches $\varphi_{max} = 1/G_{eff}\alpha_s(q'^2)\langle q_{Rt}^2 \rangle$, the diagrams which come into play first are the diagrams of Fig. 4a. We have denoted the trajectory with the largest j (the lowest) on which φ reaches the value φ_{max} by 3 in Fig. 1. This curve bounds the region in which the contributions of the multiladder diagrams are small and the results of the calculations made in the previous section are valid. Above curve 3, the semienhanced graphs of Figs. 4a and 4c, which determine the main corrections due to rescattering and screening of the partons, significantly change the behavior of the structure functions $D(\omega, q^2)$.

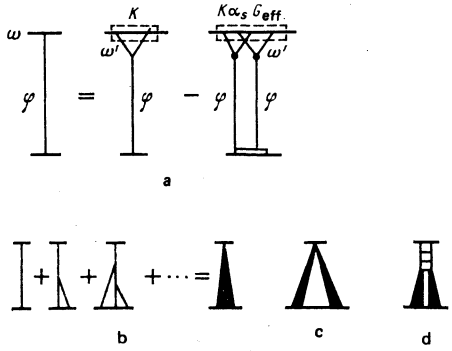

FIG. 5.

2. The method of summation

Since for $\alpha_s \varphi \sim R_{tg}^2/G_{eff}$ the contributions of the ladder (Fig. 2a) and various semienhanced diagrams of Figs. 4a and 4c are comparable, to calculate the structure function D above curve 3 it is necessary to find the sum of all diagrams of the type of Fig. 4c. This task can be done by means of the equation (see Fig. 5)

$$\frac{\partial \varphi(\ln \omega', r)}{\partial \ln \omega'} = \int \bar{K}(q^2, q'^2)\varphi(\ln \omega', r')[1 - \alpha_s(q^2)\varphi(\ln \omega', r) \times G_{eff}\langle q_{Rt}^2 \rangle/16\pi^2] \frac{4N\alpha_s(q'^2)}{4\pi} dq'^2. \quad (20)$$

Here, the first term (the unity in the square brackets) describes symbolically the basic system of ladder equations (2). This becomes completely obvious if we retain in Eqs. (2) only the first term and note that in the j representation the derivative $\partial\varphi/\partial \ln \omega$ corresponds to $(j-1)\varphi(j)$ (in this special case, $\hat{K} = K$). The second term in the square brackets corresponds to the contribution of the semi-enhanced diagram in Fig. 4a, i.e., J_{4a} (19). Since this term takes into account the possibility of coalescence of ladders at each level of the rapidities $\ln \omega'$, and the function φ itself at smaller values of ω' was calculated earlier by means of this equation, it follows that Eq. (20) thus generates the entire fan of the semi-enhanced graphs of Fig. 4c.

Indeed, if at the level $\ln \omega'$ we have already specified the sum of the diagrams of Fig. 5b [i.e., $\varphi(\ln \omega')$], then, iterating (20) by means of the second term, we obtain a new, as yet unenhanced diagram Fig. 5c, and, using in the subsequent iterations the first term, we transform this graph into the semi-enhanced Fig. 5d and so forth. The initial condition for Eq. (20) is the function $\varphi(\omega_0, q^2)$ calculated in the usual manner[1,2] by summing the leading logarithms of the transverse momentum at finite ω_0. In the case $1 \ll \ln \omega_0 \ll 1/\alpha_s(q_0^2)$,

$$\varphi(\omega_0, q^2) \propto \frac{1}{q^2} \exp\left[\frac{16N}{\beta_2} \ln \omega_0 \ln \ln q^2\right]^{1/2}. \quad (21)$$

However, since we must now impose the initial condition for fixed ω_0, we must, in solving Eq. (20), specify $\varphi(\omega_0, q^2)$ and then calculate $\varphi(\omega, q^2)$ for all values of q^2, including $q^2 < q_0^2$, where $\alpha_s(q^2) \gtrsim 1$ and our equations of the leading logarithmic approximation no longer work. To avoid this problem, we must, besides the initial condition $\varphi(\omega_0, q^2)$, impose an initial condition for $\varphi(\omega, q^2)$ on some curve $q^2 = F(\omega) > q_0^2$ [curve 2 in

Fig. 1, to the right of which $\alpha_s(q^2) < \alpha_s(q_0^2) \ll 1$]. The formulation of such a boundary condition is our next task.

Below, investigating Eq. (20), we shall succeed in finding a curve 2 on which $\varphi(\omega(q^2), q^2) = \text{const}$. Everywhere to the left of curve 2 ($\omega > \omega(q^2)$) the function φ is so large that, besides the semienhanced diagrams, we should also take into account the contributions of the completely enhanced graphs. This is a very complicated problem, and we shall not attack it here. However, on the boundary 2 itself and to the right of it [$\omega \leqslant \omega(q^2)$, $\varphi \leqslant \text{const}$] the contribution of the multiladder diagrams (the cuts) to Eq. (20), $O(\alpha_s\varphi) < O(\alpha_s)$, becomes negligibly small. This makes it possible to return to the basic system of linear equations (2) and, imposing the boundary condition on curve 2, $\varphi(\omega(q^2), q^2) = \text{const}$, find the structure functions in the entire region C to the right of the boundary.

Thus, the role of the cuts reduces to the imposition of a new boundary condition (at large ω and q^2) in the old ladder equations (2).

3. Investigation of the nonlinear equation (20)

We now return to Eq. (20), which sums the semienhanced graphs. In the first part of this section, we showed that the multipomeron cuts (Figs. 4a and 4d) have a significant influence on the behavior of the functions φ only when the cross sections $\alpha_s\varphi(\omega', q'^2) \gtrsim 1/\langle q_{Rt}^2 \rangle$ are sufficiently large [see also Eq. (20)]. On the other hand, writing $\varphi(\omega, q^2)$ in the form of the integral (12), we have seen that once the saddle-point value f_0 becomes less than 0.37 the function φ begins to decrease rapidly with increasing q^2. Therefore, in the region where the cross sections $\alpha_s\varphi \sim 1/\langle q_{Rt}^2 \rangle$ are not small and it is necessary to sum the semi-enhanced diagrams the functions $\varphi(\omega', q'^2)$ themselves still vary comparatively slowly with q'^2, $\varphi \propto q^{2f-1}$, $f \approx f_0$. All the integrals over q'^2 in Eqs. (2) and (20) converge well at $q' \sim q$, and they do not contain the $\ln q^2$ that arose earlier because of the contribution of the states (eigenfunctions φ_f) with $f \to 0$.

As a result, studying the influence of the cuts, we can retain in the system (2) only the part singular in j (i.e., the first term) and interpret Eq. (20) literally, i.e., not as a system of equations for φ_F and φ_G but as a single equation for the function $\varphi = \varphi_G$ with kernel $\hat{K} = K$ given by the expression (3).

Since in the initial condition (and, as we hope, in the final solution) the slope $k = -\partial \ln \varphi / \partial \ln q^2$ varies slowly with q^2, and the integrals (20) over q' converge rapidly, we write φ in the form of the exponential

$$\varphi(\ln\omega, q'^2) = \varphi_0(\ln\omega, q^2) e^{k(r-r')} \quad (r' = \ln q'^2)$$

and follow how φ_0 and the slope $-k$ change with increasing ω.

To find the equation for k, we differentiate (20) with respect to $\partial r = \partial \ln q^2$:

$$\frac{\partial k}{\partial \ln\omega} = \frac{\partial}{\partial \ln\omega}\left(-\frac{1}{\varphi}\frac{\partial\varphi}{\partial r}\right) = -\frac{\partial^2\varphi}{\varphi\,\partial r\,\partial\ln\omega} - \frac{k}{\varphi}\frac{\partial\varphi}{\partial\ln\omega}$$
$$= \frac{4N\alpha_s}{4\pi}\chi(1-k)\left\{\frac{1-\varphi/\varphi_{max}}{r} - \frac{k\varphi}{\varphi_{max}}\right\} + \frac{4N\alpha_s}{4\pi}\left[1-\frac{\varphi}{\varphi_{max}}\right]\chi'(1-k)\frac{\partial k}{\partial r}. \quad (22)$$

We have here denoted by $1/\varphi_{max}$ the coefficient of φ in the square brackets of the integral (20), $\varphi_{max} = 16\pi^2/G_{eff}\langle q_{Rt}^2 \rangle \alpha_s(q^2)$, and we have retained in all the terms of the right-hand side of (22) only the leading terms in $1/r$.

For the following study of the obtained system (20), (22) it is convenient to use the analogy with the optical wave equation. For the field φ, we introduce the following concepts: the frequency

$$\tilde{\omega} = \frac{\partial \ln\varphi}{\partial\ln\omega} = \frac{4N\alpha_s}{4\pi}\chi(1-k)[1-\varphi/\varphi_{max}] \quad (23)$$

[see (20)] and the wave vector $k = -\partial\ln\varphi/\partial r$. Then, moving with the group velocity

$$\left.\frac{dr}{d\ln\omega}\right|_{gr} = v_{gr} = \frac{\partial\tilde{\omega}}{\partial k} = \frac{-4N}{\beta_2 r}[1-\varphi/\varphi_{max}]\chi'(1-k), \quad (24)$$

we can readily follow the variation of the wave vector k, since now Eq. (25) for $dk/d\ln\omega|_{gr}$ does not contain the derivative $\partial k/\partial R$:

$$\left.\frac{dk}{d\ln\omega}\right|_{gr} = \frac{\partial k}{\partial\ln\omega} + v_{gr}\frac{\partial k}{\partial r} = \frac{4N\alpha_s}{4\pi}\chi(1-k)\left[\frac{1-\varphi/\varphi_{max}}{r} - \frac{k\varphi}{\varphi_{max}}\right]. \quad (25)$$

In other words, moving with the group velocity, we follow the same wave packet the whole time and must not take into account the changes in the slope of φ associated with the distribution of the wave packets given by the initial condition (21). However, it is much easier to follow the value of φ on a trajectory determined by the phase velocity:

$$v_{ph} = \frac{\tilde{\omega}}{k} = \left.\frac{dr}{d\ln\omega}\right|_{ph} = \frac{4N}{\beta_2 r}\left[1-\frac{\varphi}{\varphi_{max}}\right]\frac{\chi(1-k)}{k}. \quad (26)$$

Along this trajectory, the value of φ is constant. It is here necessary to emphasize the serious difference between our reggeon equation (20) and the usual wave equation. Since the rapidity $\ln\omega$ in reggeon field theory plays the part of an imaginary time, it, the change in the phase $\Delta\psi = i(v - v_{ph})i\Delta\ln\omega$ when the velocity of motion v differs from v_{ph} leads to a sharp change in the value of the function $\Delta\ln\varphi = (v_{ph} - v)\Delta\ln\omega$.

As can be seen from Eqs. (20) and (23), the values of $\varphi(\ln\omega, q^2)$ increase monotonically with increasing $\ln\omega$, drawing closer to the value φ_{max} but nowhere exceeding it, i.e., $1 - \varphi/\varphi_{max} > 0$. Simultaneously, it follows from Eq. (25) that the slope k is everywhere positive (for $k \leqslant 0$, $dk/d\ln\omega|_{gr} > 0$, and in the initial condition $k > 0$). Hence, for fixed $\ln\omega$ the function $\varphi(\omega, q^2)$ decreases monotonically with increasing q^2. The behavior of the vector k is more complicated. If we begin with a wave packet for which $v_{gr} > v_{ph}$ (i.e., $f_0 = 1 - k > 0.37$), then in the case of motion with the velocity v_{gr} the ratio φ/φ_{max} will rapidly decrease and, in accordance with Eq. (25), the value of k will increase, making the ratio v_{gr}/v_{ph} still larger. The problem linearizes, and in this region we can use the old system (2) for the calculations. In the opposite initial case, $v_{gr} < v_{ph}$ (i.e., $1 - k > 0.37$), the value of φ increases rapidly, tending to φ_{max}. In Eq. (25), the last term $-k\varphi/\varphi_{max}$ begins to play the main part, and the vector k on such a group trajectory decreases with increasing ω and q^2.

Of greatest interest is the intermediate case $v_{ph} = v_{gr}$, when we can readily follow the variations of k and φ_0 simultaneously. To this condition there corresponds a constant value $k = k_0$, which is the solution of the equation

$$\chi'(1-k_0)+\chi(1-k_0)/k_0=0, \quad k_0=0.63. \tag{27}$$

We join by a curve (2 in Fig. 1) the points in the $(\ln\omega)$ plane for which $k = k_0$. Generally speaking, different wave packets could pass through each point of this curve $k = k_0$. It would then be very difficult to follow the variation of φ along curve 2. But, as we shall now show, this curve is simultaneously the trajectory of motion of a packet with velocity $v_{gr} = v_{ph}$, and on it $\varphi = \text{const}$. Indeed, if curve 2 did not coincide with the packet trajectory, i.e., $dr/d\ln\omega \neq v_{gr} = v_{ph}$ along the curve, the values of φ would change on curve 2. Then one could find a point at which

$$\frac{\varphi}{\varphi_{max}} = \frac{\varphi G_{eff}\langle q_{Rt}^2\rangle}{4\pi\beta_2 r} = \frac{1}{k_0 r},$$

i.e.,

$$\varphi = \text{const} = \frac{4\pi\beta_2}{k_0 G_{eff}\langle q_{Rt}^2\rangle} = \varphi_{gr}.$$

Moving from this point with velocity $v_{gr} = v_{ph}$, we see that the derivative (25) $dk/d\ln\omega\big|_{gr}$ vanishes to our required accuracy $O(\alpha_s^3(q^2))$. Hence, moving with the velocity $v_{ph} = v_{gr}$ from the point $\varphi = \varphi_{gr}$, we move simultaneously along curve 2, keeping as before the value of φ equal to φ_{gr}.

4. Calculation of the structure functions

Thus, we have demonstrated the importance in the solution of Eq. (20) of curve 2 (Fig. 1), on which $\varphi = \varphi_{gr} = \text{const}$, and we have obtained the possibility of determining the form of this curve:

$$\frac{dr}{d\ln\omega} = v_{gr} = v_{ph} = -\frac{4N\chi'(1-k_0)}{\beta_2 r} + O(\alpha_s^2(q^2)), \tag{28}$$

i.e.,

$$\ln\omega_{gr} = 0.21\beta_2 r^2/8N = 0.42\pi^2/N\beta_2\alpha_s^2(q^2). \tag{29}$$

[Here, we have ignored the terms $\varphi_{gr}/\varphi_{max} \sim \alpha_s(q^2)$ compared with unity, since such corrections were already omitted in the calculation of the kernel K, i.e., $\chi(1-k)$.]

Since everywhere to the right of the curve 2 we have $\varphi(\omega, q^2) \leq \varphi_{gr} = \text{const}$ (the function φ decreases monotonically with increasing q^2 for fixed ω), the contributions of the cuts (Figs. 4a, 4c, and 4d) in this region is a negligibly small ($\sim\alpha_s(q^2)$) correction to the equations of the basic system (2).[5] As a result, since we are interested in the region to the right of curve 2, we can forget the multiladder diagrams and consider only the linear system (2) of equations of the leading logarithmic approximation augmented by the boundary condition $\varphi = \varphi_{gr} = \text{const}$ on the curve (29). As before, it is convenient to seek the solution of such a system in the form (12), in which for large j [for which the corresponding $\omega(q_0) < \omega_{gr}(q_0)$ (29)] the coefficients $A_0(j)$ are determined by the initial condition $\varphi_0(\omega, q_0^2)$, and for $j \to 1$ [when $\omega(q_0) \geq \omega_{gr}(q_0)$] $A_0(j)$ is given by our new boundary condition on the curve (29) (i.e., essentially it is determined by the cuts). To satisfy the boundary condition, it is necessary to choose

$$A_0(j) = \frac{\text{const}}{(j-1)^{5/6}} \exp\frac{8N\cdot 0.309}{\beta_2(j-1)}; \tag{30}$$

the number $0.309 = B$ is found by solving the equation

$$k_0\chi(1-k_0) = 2\int_{0.5}^{1-k_0}\chi(f')\,df' + 4B.$$

Thus, the behavior of the cross section of deep inelastic scattering is finally as follows: a) in the region

$$\ln\omega < \frac{0.84\pi^2\ln\ln q^2}{N\beta_2\alpha_s^2(q_0^2)}$$

(curve 3 in Fig. 1)[6] it is described by the usual formulas of the leading logarithmic approximation (2), which permit the calculations of $\varphi(\omega, q^2)$ and $D(\omega, q^2)$ from initial conditions at $q^2 = q_0^2$, and b) in the region

$$\frac{0.84\pi^2\ln\ln q^2}{N\beta_2\alpha_s^2(q_0^2)} < \ln\omega < \frac{0.42\pi^2}{N\beta_2\alpha_s^2(q^2)}$$

it is described by the expressions

$$\varphi(\omega, q^2) = \frac{\text{const}}{q^2}(\alpha_s(q^2))^{1/6}H(\varkappa)q^{2F(\varkappa)}, \tag{31}$$

($\varkappa = \beta_2 N\alpha_s^2(q^2)\ln\omega/2\pi^2$). The functions $F(\varkappa)$ and $H(\varkappa)$ are plotted in Fig. 6. Their asymptotic behaviors at small $\varkappa \ll 1$ are given by the expressions

$$F(\varkappa) = f_0 + \varkappa/f_0 + O(f_0^2), \quad H = f_0^{1/6-7}(2\ln f_0^{-1})^{1/6}; \quad H = H/f_0, \tag{32}$$

where the saddle-point value f_0 is determined by the equation

$$4f_0^2(0.309 - \ln\sqrt{f_0}) = \varkappa.$$

As $\varkappa \to 0.21$ (i.e., near curve 2 in Fig. 1, on which we specified the new boundary condition $\varphi = \varphi_{gr} = \text{const}$)[7]

$$F(\varkappa) \to 1, \quad H \propto (\alpha_s(q^2))^{-1/6}.$$

IV. CONCLUSIONS

Let us briefly formulate the main results of the paper.

1. We have obtained a system of equations that makes it possible to sum all diagrams containing at least one of the two logarithmically large parameters $\ln\omega$ and $\ln q^2$. Solving these equations, we have calculated the structure functions of deep inelastic scattering in the region

$$\ln\omega/\omega_0 < 0.84\pi^2[\ln\ln q^2 - \ln\ln q_0^2]/N\beta_2\alpha_s^2(q_0^2).$$

2. In a large region (to the right of curve 2 in Fig.

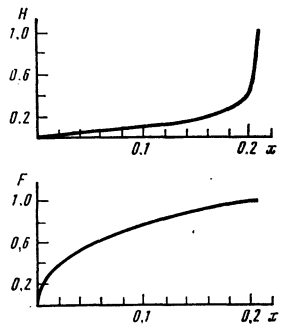

FIG. 6.

1) we have succeeded in reducing the influence of the multipomeron diagrams (cuts) to the imposition of a new boundary condition ($\varphi = \text{const}$) on curve 2 [$\ln \omega = 0.42\,\pi^2/N\beta_2\alpha_s^2(q^2)$] in the basic system of linear equations and finding in this region the structure functions up to a slowly varying pre-exponential factor. We emphasize that although the role of the cuts has been reduced to the imposition of a new boundary condition in the equations describing the sum of the ladder graphs, the cuts have radically changed the exponential behavior of the structure functions $D(\omega, q^2)$. Whereas without allowance for the multiladder graphs[1,2,11]

$$\ln\frac{D}{\omega} \approx \left(\frac{16N}{\beta_2}\ln\omega\ln\ln q^2\right)^{1/2}$$

and near curve 2, $\ln\omega \sim \ln^2 q^2$, the parton density D/ω appreciably exceeds the bound $D/\omega \propto q^2\sigma^\gamma < q^2(\ln\omega)^2$ which follows from the unitarity condition (Froissart theorem), we now have $D/\omega \propto q^{2F}$, and $F \leq 1$ to the right of the boundary (2).

Naturally, the change in the nature of the behavior of the structure functions in the region of very small $x = 1/\omega$ (hitherto suggestions have only been made concerning the form of the functions D in this region)[11] has serious consequences—on the shape of the spectrum and magnitude of the inclusive cross sections for production of hadrons with large transverse momenta in the pionization region, on the energy dependence and shape of the plateau in e^+e^- annihilation, and so forth.

We are very grateful to V. N. Gribov for discussion and constant interest in the work and to L. N. Lipatov for discussing the results.

[1)]The above proof that $\ln\omega$ is absent in the encompassing graphs is almost literally repeated in the case of a planar gauge, for example, $d_{\mu\nu} = g_{\mu\nu} - (q_\mu p_{B\nu} + p_{B\mu} q_\nu)/(qp_B)$, and here it is not even necessary to follow the canceling of the polarizations q_μ, since $p_{A\mu} d_{\mu\nu} \approx -q_{1\nu}/\alpha$. First attempts to reduce the regeization to a single cell of the ladder by the choice of a special gauge were made by Mason Ref. 7. After the present paper had been written, we became acquainted with Jaroszewicz's paper,[8] in which he showed independently that in the Coulomb gauge the infrared-divergent contributions to the gluon reggeization also reduce to graphs of the form of Fig. 2e.

[2)]We recall that the inclusion of any extra gluon in diagrams of the form of Fig. 2a lead only to corrections $\Delta K \propto \alpha_s$ in the kernels of Eqs. (2).

[3)]We call our ladders reggeons (pomerons) to preserve the usual terminology in the theory of complex angular momenta j, although the singularities corresponding to our ladder are not simple poles in the j plane.

[4)]A more detailed discussion of the procedure for calculating the integral over q_{Rt} for the example of doubly logarithmic diagrams can be found in our paper Ref. 10.

[5)]The influence of the cuts is important only for maintaining a constant value $k = k_0$ of the wave vector along the trajectory 2. Since the change in the slope k along the group trajectory in the case of the linear system (2) is an effect of second order in α_s [see (25)], the vanishing of the derivative $dk/d\ln\omega$ was guaranteed by very small contributions of the multipomeron diagrams, which need not be taken into account in any of our other calculations.

[6)]Below curve 3 the values of the parameter $\alpha_s(q^2)\varphi(\omega, q^2) \leq 16\pi^2 R_{tg}^2/G_{eff}$ are such that the contributions of the multiladder diagrams are negligibly small everywhere for $q^2 > q_0^2$ and they should be ignored even in the form of the new boundary conditions.

[7)]As was discussed in Sec. 2.4, the corrections $\sim\alpha_s$ omitted in the calculation of the ladder kernels K (3) and Φ (4) lead to a finite renormalization of the coefficients $A_0(j, f)$ in an interval of finite f. Therefore, we cannot here pretend to exact calculation of the slowly varying pre-exponential factor $H(\varkappa)$ for the region b) but merely aim to find the form of the singular part of $H(\varkappa)$ as $\varkappa \to 0$.

[1]Yu. L. Dokshitser, Zh. Eksp. Teor. Fiz. 73, 1216 (1977) [Sov. Phys. JETP 46, 641 (1977)].
[2]G. Altarelli and G. Parisi, Nucl. Phys. B126, 298 (1977).
[3]E. A. Kuraev, L. N. Lipatov, and V. S. Fadin, Zh. Eksp. Teor. Fiz. 72, 377 (1977) [Sov. Phys. JETP 45, 199 (1977)].
[4]L. V. Gribov, Nucl. Phys. B168, 429 (1980).
[5]V. V. Sudakov, Zh. Eksp. Teor. Fiz. 30, 187 (1956) [Sov. Phys. JETP 3, 115 (1956)].
[6]V. N. Gribov and L. N. Lipatov, Yad. Fiz. 15, 781 (1972) [Sov. J. Nucl. Phys. 15, 438 (1972)].
[7]A. L. Mason, Nucl. Phys. B117, 493 (1976); B120, 275 (1977).
[8]T. Jaroszewicz, Krakow Report INP-1098/PH, Krakow, June (1980).
[9]Yu. L. Dokshitzer, D. I. Dyakonov, and S. I. Troyan, Phys. Rep. 58C, 296 (1980).
[10]L. V. Gribov, E. M. Levin, and M. G. Ryskin, Nucl. Phys. B (in press).
[11]Chi-Min Wu, Nucl. Phys. B167, 337 (1980).

Translated by J. B. Barbour